Jurnal
Teknologi

Full Paper

VENTILATION PERFORMANCE OF DIFFERENT TYPES OF MIXING VENTILATION SYSTEMS IN A GENERIC SCALED-DOWN EMPTY AIRCRAFT CABIN

Shahliza Azreen Sarmin[a,b], Azli Abd Razak[b*], Fauziah Jerai[b], Mohd Khir Harun[a]

[a]Malaysian Institute of Aviation Technology, Universiti Kuala Lumpur, 43800 Dengkil, Selangor, Malaysia
[b]School of Mechanical Engineering, College of Engineering, Universiti Teknologi MARA, 40450 Shah Alam, Selangor, Malaysia

Article history
Received
8 March 2024
Received in revised form
24 July 2024
Accepted
9 October 2024
Published Online
20 February 2025

*Corresponding author
azlirazak@uitm.edu.my

Graphical abstract

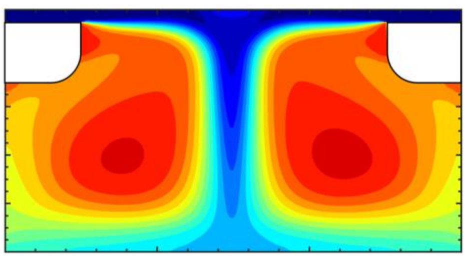

Abstract

The ventilation system of a commercial aircraft cabin plays an important role in ensuring passenger comfort and health during the flight. The commonly utilized ventilation system in aircraft cabin is mixing ventilation, where air is supplied either through the ceiling or sidewalls. However, ventilation efficiency can be affected by different types of mixing ventilation systems. Therefore, this study aims to evaluate airflow distribution and ventilation performance of various types of mixing ventilation systems, namely ceiling ventilation (CV), sidewall ventilation (SV), and the combination of ceiling and sidewall ventilation (CSV) of a generic scaled-down empty aircraft cabin. Computational Fluid Dynamics (CFD) with Launder-Sharma Low Reynold Number (L-S LRN) turbulence model using Open-source Field Operation and Manipulation (OpenFOAM) software was utilized in this simulation. For all simulated cases, two large circulation regions were observed on both sides of the aircraft cabin, with CV depicted a greater size of circulation compared to other ventilation approaches. The velocity profiles clearly showed the difference between the three ventilation systems, particularly in the merged jet area. Furthermore, different type of ventilation system affects the distribution of the age of the air in the aircraft cabin. The ceiling supplemented with the sidewall mixing system or CSV is able to reduce the age of the air, indicating that it has better ventilation efficiency.

Keywords: Aircraft cabin, mixing ventilation, CFD, OpenFOAM, ventilation performance

Abstrak

Sistem pengudaraan di dalam kabin pesawat komersial memainkan peranan penting dalam memastikan keselesaan dan kesihatan penumpang semasa penerbangan. Sistem pengudaraan yang biasa digunakan di dalam kabin pesawat adalah pengudaraan campuran, di mana udara dimasukkan melalui siling atau dinding sisi. Walau bagaimanapun, kecekapan pengudaraan boleh dipengaruhi oleh sistem pengudaraan campuran yang berbeza. Oleh itu, kajian ini bertujuan untuk menilai taburan aliran udara dan prestasi pengudaraan pelbagai jenis sistem pengudaraan campuran, iaitu pengudaraan melalui siling (CV), pengudaraan melalui dinding sisi (SV), dan gabungan pengudaraan melalui siling dan dinding sisi (CSV) di dalam sebuah model kabin pesawat kosong yang berskala kecil. Computational Fluid Dynamic (CFD) dengan model Launder-Sharma (L-S LRN) menggunakan perisian Open-source Field Operation and Manipulation (OpenFOAM) digunakan dalam simulasi ini. Dalam semua kes simulasi, dua kawasan peredaran besar diperhatikan di kedua-dua belah sisi kabin pesawat, dengan CV menunjukkan saiz peredaran yang lebih besar berbanding pendekatan pengudaraan lain. Profil halaju juga dengan jelas menunjukkan perbezaan antara tiga sistem pengudaraan, terutama di kawasan aliran gabungan. Selain itu, jenis sistem pengudaraan yang berbeza mempengaruhi taburan umur udara di dalam kabin pesawat. Pengudaraan gabungan antara siling dan dinding sisi atau dikenali CSV dapat mengurangkan umur udara seterusnya menunjukkan ia mempunyai kecekapan pengudaraan yang lebih baik di antara pengudaran yang lain.

Kata kunci: Kabin pesawat, pengudaraan campuran, CFD, OpenFOAM, kecekapan pengudaraan

1.0 INTRODUCTION

With rapid technological and economic development, commercial aircraft has become a viable means of transport in modern society, carrying billions of passengers around the world every year. As more passengers choose to travel by air, there is greater concern over thermal comfort and safety in aircraft cabins due to the high passenger density.In addition, the transmission of contaminants through air travel is a major health concern due to the outbreak of the SARS-CoV-2 pandemic [1]–[3]. Investigating the spread mechanism within the aircraft cabin is of utmost importance. Therefore, a comprehensive study is imperative to investigate the air distribution and ventilation efficiency in the confined aircraft cabin.

Mixing ventilation system is currently widely used in aircraft cabin, where both fresh air and recirculated air are supplied either from the ceiling or from the side wall under the baggage compartment and then discharged from the side wall near the floor [4]. This system comprises various positioning of air supplies such as at ceiling, side wall and both of ceiling and side wall. Typically, personal gaspers are coupled to each of these vents to provide fresh air directly into the specific regions of each traveller [5].

Numerous experimental and numerical studies have used the above ventilation system as the primary system of interest. Li *et al.* [6] conducted an experimental study in an aircraft cabin model using two-dimensional particle image velocimetry. Measurements for three distinct orientations of air distribution, namely cross-sectional, horizontal, and longitudinal were performed. The findings indicated that although the airflow patterns in various cross-sections displayed inconsistencies, significant similarities were also noted.

Zhang *et al*. [7] conducted an experimental study with an aircraft cabin mock-up to assess the effectiveness of different ventilation systems, namely ceiling ventilation (CMV), sidewall ventilation (SMV), and ceiling and sidewall ventilation (CSMV). With SMV, two large circulation patterns were observed in the aisle area. In the CSMV, the velocity of large-scale circulation was weakened, while at the same time, the velocities in the aisle area decreased. However, a higher velocity was observed in the aisle region of CMV. In addition, CMV resulted in more significant heat accumulation due to large-scale circulation compared to SMV and CSMV. The study also conducted a comparative analysis of the velocity non-uniformity index (VNUI), temperature non-uniformity index (TNUI), and heat removal efficiency of different ventilation systems in the cabin. The results showed that the CSMV demonstrated the highest performance in VNUI and age of air.

In a separate investigation, You *et al.* [4] assessed three different ventilation systems (mixing, conventional displacement, and personalized displacement) in Boeing 737 and 767 aircraft models, assessing contaminant infection risk using the Wells-Riley approach. They found the mixing system exhibited a higher infection risk compared to the displacement systems. Liu *et al.* [8] used VNUI, TNUI, mean age of air, draft rate, and percentage dissatisfaction to evaluate the comfort level in both systems in order to assess mixing and displacement ventilation comfort levels in a mock aircraft cabin. While the mixing system displayed more uniform velocity and temperature, the mean age of air did not significantly differ between systems. However, in an earlier experimental investigation by Wang *et al.* [9], it was revealed that the local mean age of air is greatly influenced by different ventilation strategies.

Consequently, investigating the age of air is significant since it serves as a crucial indicator for assessing the effectiveness of ventilation in a confined area. Although mixing ventilation in aircraft cabin has been extensively researched (Ref. [6]–[14]), a comprehensive understanding of the fundamental flow components remains limited. The in-depth study of these fundamental flow characteristics holds significant potential for optimising the design of mixing ventilation. Therefore, using a scaled-down model could provide comprehensive information about the entire complex flow field and make more accurate predictions than a full-scale complex model or experiment. In addition, different mixing ventilation systems could affect the ventilation efficiency [7].

A prior investigation confirmed the accuracy of computational fluid dynamics (CFD) simulations in representing airflow patterns in a scaled-down empty model of an aircraft cabin with ceiling mixing ventilation. Additionally, the study identified appropriate turbulence models for precise modeling. The current study examines the airflow velocity and ventilation efficiency of several types of mixing ventilation systems, including the ceiling mixing ventilation system (CV), sidewall mixing ventilation system (SV), and ceiling sidewall mixing ventilation system (CSV). The performance of each type of mixing ventilation system is assessed through the evaluation of the velocity contour and vector, velocity profiles, and the age of air.

2.0 METHODOLOGY

2.1 Numerical Simulation Settings

2.1.1 Verification and Validation

Sarmin *et al.* [15] performed a selection of turbulence models utilizing the Open Field Operation And Manipulation (OpenFOAM) software and three closure models: renormalization group k-ε (RNG), realizable k-ε (RLZ), and Launder Sharma low-Reynolds number (LS-LRN). The findings indicated that the LS-LRN model exhibits superior accuracy in predicting mean velocities and turbulent kinetic energy in comparison to the other two models. In addition, a grid sensitivity analysis was performed on coarse, medium, and fine grids. The results indicated that the medium grid predicted the flow fields with excellent accuracy, as the grid convergence index (GCI) over the five vertical lines evaluated ranged from 1% to 2.19%. Hence, the LS-LRN model with a medium grid configuration is applied to various types of cabin ventilation modes in this study. Details of the verification and validation studies are referred to Ref. [15].

2.1.2 Computational Domain and Grids

Measurements made in a scaled-down of 1:11 water-filled aircraft cabin setup as reported by Thysen *et al.* [16], [17] are selected for the CFD simulation in the current study. The computational domain has a size of 300 mm x 300 mm x 200 mm for length (*L*), width (*W*), and height (*H*), as shown in Figure 1 (a). The ceiling inlets are positioned at both sides of the top domain while the sidewall inlets are located below the two cuboids with rounded ends, i.e., the baggage compartment, where the height of each inlet, h_{CFD}, is 30 mm (0.15*H*). The inlet height before entering the aircraft cabin, *h* is 10 mm (0.05*H*). The two outlets are located on both sides near the floor with a height of 20 mm (0.1*H*). The computational grid, consisting of over 14 million cells (medium) of hexahedral, prismatic, and polyhedral was created using the *blockMesh* application in OpenFOAM as illustrated in Figure 2. This medium grid was selected among the coarse grid of 682,328 cells and the fine grid of 19,305,359 cells.

In this study, three different types of mixing ventilation systems are employed; CV, SV, and CSV as shown in Figure 3. The CV supplies air from both ceiling inlets, the SV supplies air from both sidewall inlets and the CSV supplies air from both ceiling and sidewall inlets with fixed outlets. In addition, in the case of CSV, the 50:50 ratios are applied to the volumetric flow rate of the ceiling and sidewall inlets.

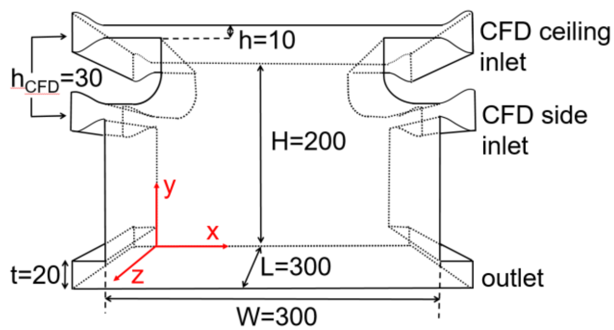

Figure 1 Computational domain (dimension in mm)

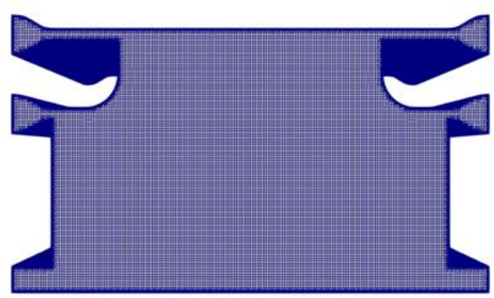

Figure 2 Computational grid for the medium grid (14 208 966 cells)

2.1.3 Boundary Conditions and Solver Settings

In this simulation, the air is used as the fluid medium where the air velocity at the position of the inlets is determined by applying the similarity theory of Reynolds (*Re*) number. At the inlets, a velocity inlet of 1.515 ms^{-1} is imposed for CV and SV cases, while 0.7575 ms^{-1} is adopted for the CSV case which corresponds to the volumetric flow rate for all simulated cases. The turbulent kinetic energy, *k* is calculated as Equation (1), while the turbulence dissipation rate *ε* is estimated as Equation (2).

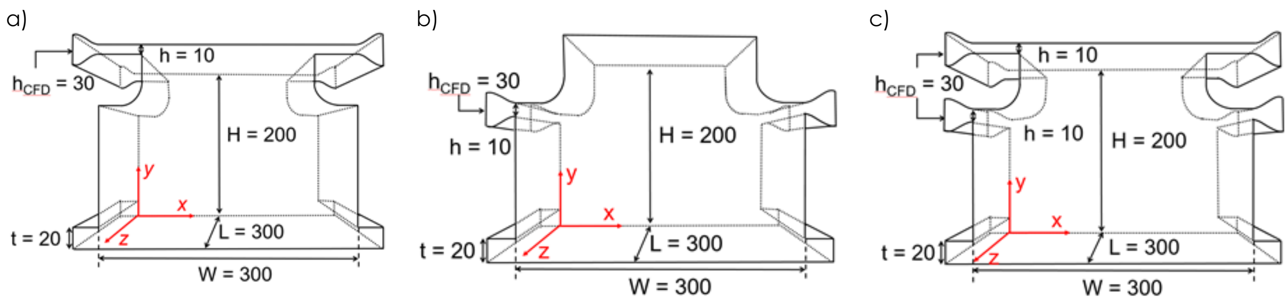

Figure 3 Computational domain of (a) CV (b) SV and (c) CSV (dimensions in mm)

$$k = 1.5(IU)^2 \tag{1}$$

$$\varepsilon = \frac{C_\mu^{\frac{3}{4}} k^{\frac{3}{2}}}{l} \tag{2}$$

where I depicts the turbulence intensity (15%) [18], U is the velocity at the inlet position, C_μ is a constant (0.09) [19] and l is the turbulent length scale which is determined by the hydraulic diameter ($2h_{CFD}L/(h_{CFD}+L)$). Static gauge pressure is set to zero at the outlet (OpenFOAM: *fixedValue, uniform 0*) and no-slip condition (OpenFOAM: *fixedValue, uniform (0 0 0)*) is applied at the cabin wall. The simulation is considered Newtonian, incompressible, and isothermal.

Table 1 shows a summary of the boundary conditions for the numerical simulation of three different mixing ventilation systems. OpenFOAM software is used to perform numerical simulation using a three-dimensional, steady Reynolds Averaged Navier-Stokes (RANS) approach. The LS-LRN turbulence model by [19] is employed using the finite volume method. The Semi-Implicit Method for Pressure Linked Equations Consistent (SIMPLEC) algorithm is used for pressure-velocity coupling. The gradient terms are discretised by a *Gauss linear* scheme while *Gauss limited linear 1* scheme is used for the divergence of all governing equations. The minimum residual threshold of 10^{-5} is implemented for all variables to monitor simulation convergence.

Table 1 Boundary conditions in the LS-LRN simulation

Boundary	CV	SV	CSV
Velocity inlet at ceiling inlets, U	1.515 ms^{-1}	Wall	0.7575 ms^{-1}
Velocity inlet at sidewall inlets, U	Wall	1.515 ms^{-1}	0.7575 ms^{-1}
Turbulence intensity, I	15%	15%	15%
Outlet	Zero static pressure	Zero static pressure	Zero static pressure
Walls	No-slip	No-slip	No-slip
Thermal conditions	Isothermal	Isothermal	Isothermal

2.2 Mean Age of Air

Mean age of air (AoA) is the mean duration that the air remains within enclosed or confined spaces before leaving to the outdoor [20]. It is an important parameter for assessing air quality or the effectiveness of ventilation and removal of contaminants. To obtain the local mean age of age (LMA), a scalar transport equation (Equation 3) is solved numerically.

$$\nabla \cdot (\mathbf{u}\tau) - \nabla \cdot (D + \frac{\nu_t}{Sc_t})\nabla\tau = 1 \tag{3}$$

where τ represents the age of air, $\mathbf{u}$ is the velocity vector with u, v and w are the velocity components of x, y, and z axis, respectively. D is the molecular diffusivity (1.5×10^{-5} m^2s^{-1}), ν_t is eddy viscosity and Sc_t is the turbulent Schmidt number ($Sc_t = 0.7$) [21]. In the AoA calculation, the boundary conditions are set to 0 at the inlet and outlet openings. *Gauss limited linear 1* scheme is adopted for the divergence while *Gauss linear corrected* scheme is applied for the laplacian terms of the scalar transport equation. The simulation of the AoA is carried out after the convergence of the SIMPLEC simulation. Therefore, the time for the AoA simulation is even shorter compared to the SIMPLEC simulation as obtained from the previous study [22].

3.0 RESULTS AND DISCUSSION

3.1 Airflow Pattern

Figure 4 illustrates the contours and vectors of the dimensionless velocity magnitude, U_{mag}/U_{max} in the midplane of x-y plane at z/H = 0.75 for the three types of mixing ventilation systems. U_{max} is defined as the average maximum magnitude of the inlet velocity just before entering the aircraft cabin. For CV and CSV (Figure 4 (a) and (c)), the air flows from the opposing inlets to the centre of the aircraft cabin and merges before changing the direction towards the cabin floor. Near the floor, the airflow is split into two streams moving to the outlets with some of the flows creating a symmetry circulation at both sides of the cabin with a different size. The CV has the largest circulation among the others.

However, in the SV case, the jets converge at a location that is shifted from the center of the cabin, specifically towards the right side. The apparent existence of the Coanda effect, caused by the curved shape of the baggage compartments located directly above the inlets, may explain this phenomena, which leads to instability in the numerical solution [6] [23]. Thus, it is worth to further investigate this finding through experiments and CFD approaches.

3.2 Air Velocity

Figures 5 and 6 show the vertical profiles of normalized mean x-velocity u (ms^{-1}) and mean y-velocity v (ms^{-1}) at the centre of the aircraft cabin (z/H = 0.75) for five (5) vertical lines, x/H = 0.13, 0.38, 0.75, 1.12 and 1.37, respectively. For the mean x-velocity profile (Figure 5) at x/H = 0.13 and 0.38, SV and CSV depict a similar pattern in the jet region, but at y/H < 0.4 region, the CSV shows a steep gradient. At x/H = 0.75, SV shows a positive value between $0.35 \leq y/H \leq 0.8$ since the evidence of the flow from the left is more dominant; while for CV and CSV, the velocity ratio is almost zero. This agrees well with the results of the airflow pattern in previous section (Figure 4) in which the SV merges more on the right side of the aircraft cabin.

At x/H = 1.12 and 1.37, the velocity profiles of CV and CSV show a similar pattern in the ceiling jet region. However, a slight difference can be seen in the velocity profile of SV and CSV in the area of the sidewall jets. Furthermore, the profile at y/h < 0.4 shows a slightly different pattern. For the mean y-velocity profile (Figure 6), the velocity profiles at x/H = 0.13 and 1.37 show a clearly similar pattern. However, at x/H = 0.38, the SV obviously shows a positive value. In the area of the merged area (z/H = 0.75), the SV also shows a more positive value.

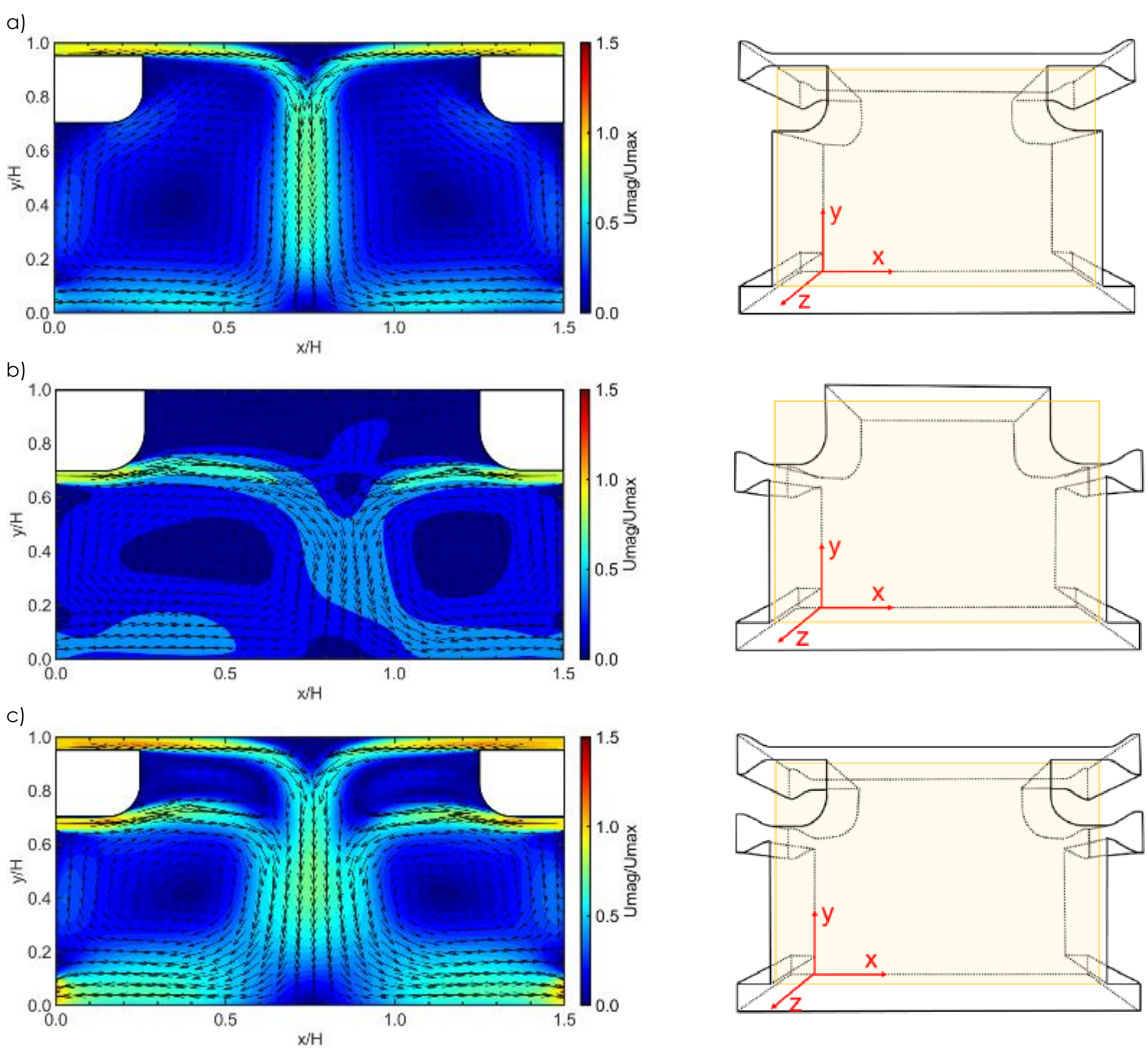

Figure 4 Contours of normalized mean velocity magnitude, U_{mag}/U_{max} in the x-y plane (z/H = 0.75) (a) CV (b) SV and (c) CSV

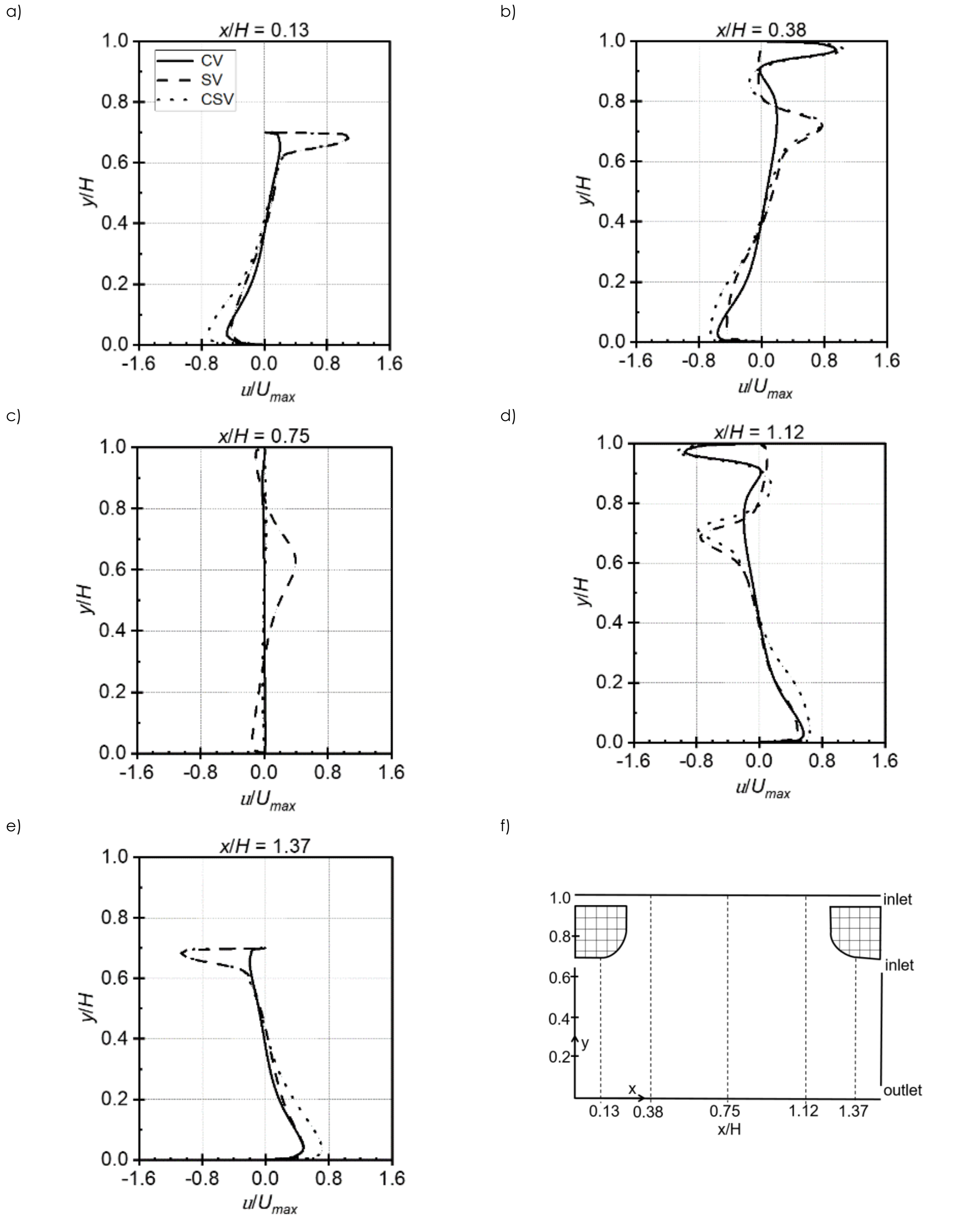

Figure 5 Normalized mean x-velocity profile, u/U_{max} at five vertical lines at plane x-y, z/H = 0.75 as shown in (f). CV: solid line, SV: dash line, CSV: dot line

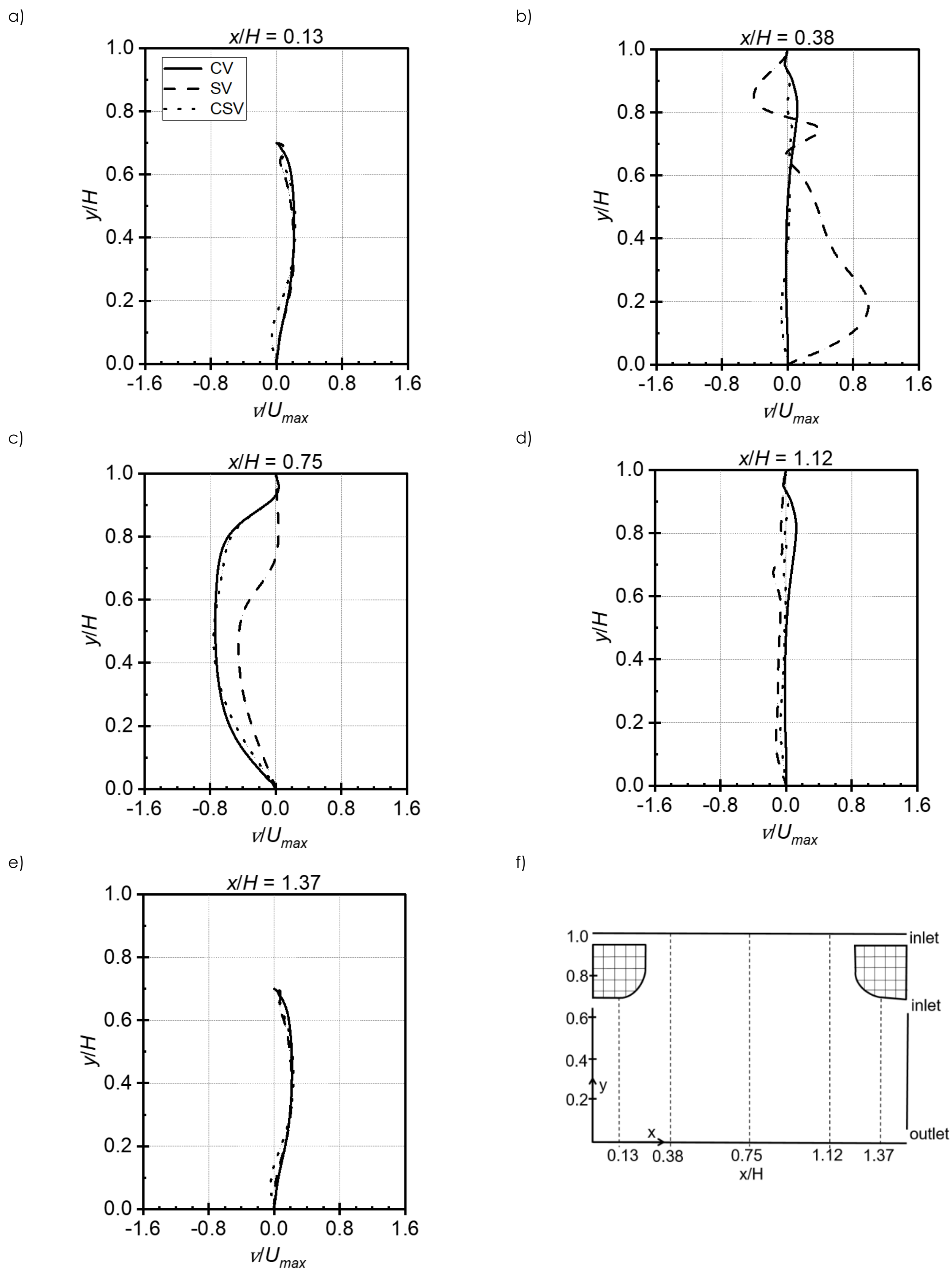

Figure 6 Normalized mean y-velocity profile, v/U_{max} at five vertical lines at plane x-y, z/H = 0.75 as shown in (f). CV: solid line, SV: dash line, CSV: dot line

3.3 Age of air

Due to the different configurations of ventilation systems, the dimensionless age of air is introduced to effectively compare the ventilation efficiency [22]. The normalized age of air can be calculated using Equation (4).

$$\bar{\tau} = \frac{\tau}{V/Q} \tag{4}$$

where V is the volume of air in the aircraft cabin and Q is the volumetric flow rate through the cabin.

Figure 7 shows the normalized age of air ($\bar{\tau}$) in the vertical plane (a-1~c-1) at z/H = 0 and horizontal plane which represent the breathing zone (a-2~c-2) at y/H = 0.5, respectively. Figure 7(a-1) depicts fresh air ($\bar{\tau} < 0.5$) near the ceiling is caused by the jet flows from the inlets and convergence of the jets contributes to relatively fresh air in the vertical area of the cabin. In the horizontal plane (Figure 7(a-2)), fresh air can be observed in the middle region which represents the aisle area, and higher age of air areas is developed on both sides that derive from the flow circulation (Figure 4(a)).

In the SV case, fresh air is observed at 0.65 ≪ y/H ≪ 0.7 as shown in Figure 7(b-1). The age of air is also relatively fresh in the convergence region of the flows from the inlets, but slightly to the right of the aircraft cabin. However, an uneven distribution age of air with a higher age of air at the left side of the aircraft cabin can be seen in the horizontal plane due to the asymmetric flows of the circulation (Figure 7(b-2)).

Figure 7(c-1) shows that the CSV has a fresh air region that covers the upper part of the cabin (baggage area to the ceiling) as a result of introducing inlets at different heights. At both sides of the cabin (Figure 7(c-2)), the age of air is improved ($0.75 \ll \bar{\tau} \ll 1.5$) while the fresh air region becomes wider at the aisle area as compared to the CV configuration. In overall, it can be concluded that the CSV provides more fresh air compared to CV and SV, which proves that CSV can provide better ventilation.

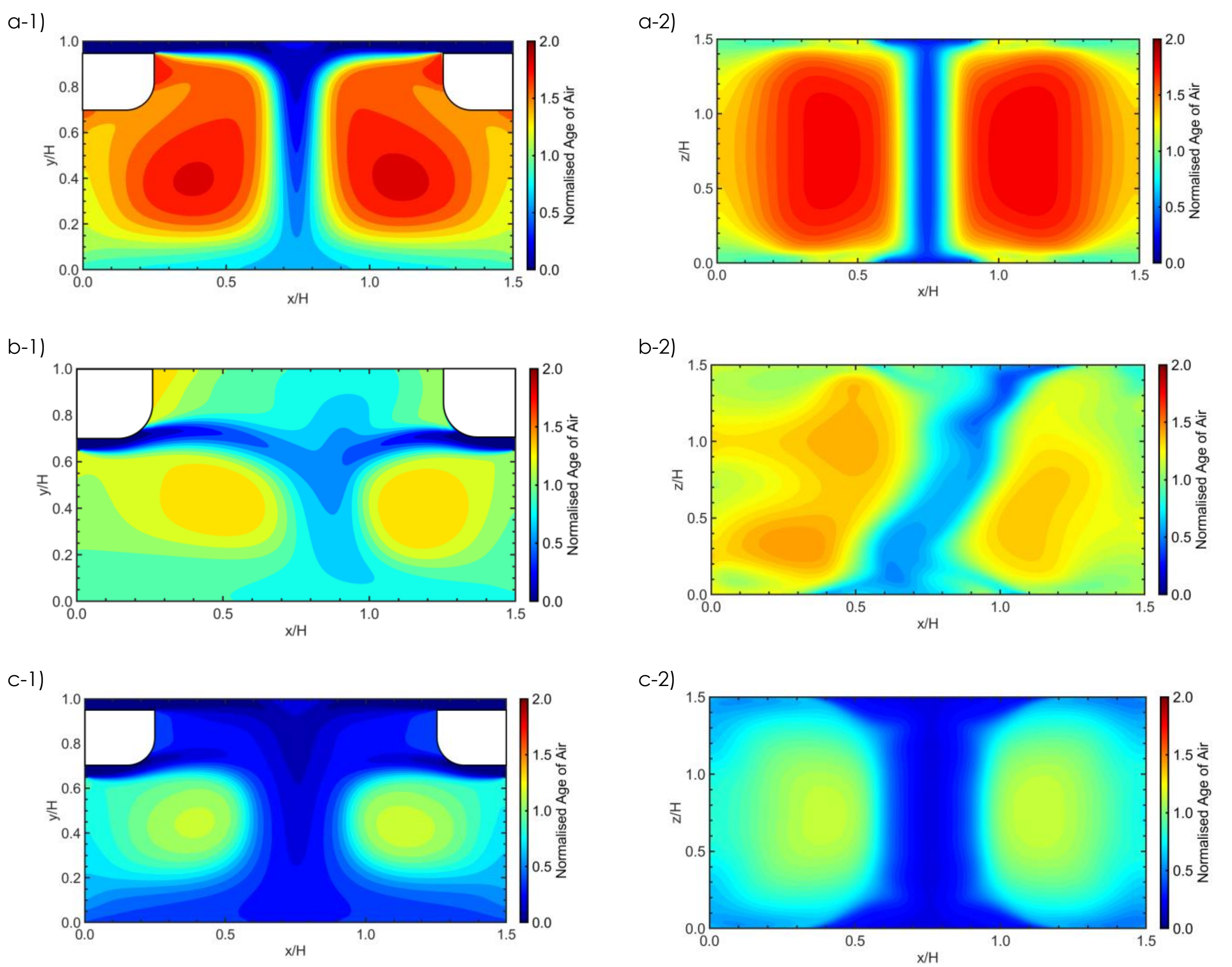

Figure 7 Normalized age of air for (a) CV (b) SV and (c) CSV for (1) *x-y* plane at *z/H* = 0.75 and (2) *x-z* plane at *y/H* = 0.5

4.0 CONCLUSION

In this study, the airflow distribution and ventilation performance in different types of mixing ventilation systems of CV, SV, and CSV are investigated in a generic scaled-down empty aircraft cabin. To perform this simulation, steady RANS model is used with the LS-LRN closure model in OpenFOAM software. Two large areas of circulation are observed on both sides of the aircraft cabin, with CV having a larger circulation compared to the other ventilation methods. However, an asymmetric pattern with flows more on the right side is observed at SV which might be due to the numerical instability. The velocity profiles clearly exhibit the differences among the three ventilation systems, especially in the area of the merged jet. Furthermore, the type of ventilation system employed has an influence on the distribution of the age of the air in the aircraft cabin. The implementation of a ceiling and sidewall mixing system (CSV) results in significant improvements in the age of air, suggesting that it offers better ventilation efficacy. Given that the present investigation only examined a 50:50 volumetric flow rate ratio for CSV, subsequent research may also explore into alternative volumetric flow rate ratios and displacement ventilation systems.

Acknowledgement

The authors express gratitude to Universiti Kuala Lumpur for the invaluable support extended to the primary author while pursuing doctoral studies at the School of Mechanical Engineering, College of Engineering, Universiti Teknologi MARA (UiTM) Shah Alam.

Conflicts of Interest

The author(s) declare(s) that there is no conflict of interest regarding the publication of this paper.

References

[1] Kelly, D., Bambury, N., Boland, M. 2021. In-flight Transmission of Wild-type SARS-CoV-2 and the Outbreak Potential of Imported Clusters of COVID-19: A Review of Published Evidence. *Globalization and Health. 17*(1): 1–5. Doi: https://doi.org/10.1186/s12992-021-00749-6.

[2] Bielecki, M., Patel, D., Hinkelbein, J., Komorowski, M., Kester, J., Ebrahim, S., Rodriguez-Morales, A. J., Memish, Z. A., Schlagenhauf, P. 2020. Reprint of: Air Travel and COVID-19 Prevention in the Pandemic and Peri-pandemic Period: A Narrative Review. T*ravel Medicine and Infectious Disease*. 38: 101939. Doi: https://doi.org/10.1016/j.tmaid.2020.101939.

[3] Kong, B., Zou, Y., Cheng, M., Shi, H., Jiang, Y. 2022. Droplets Transmission Mechanism in a Commercial Wide-body Aircraft Cabin. *Applied Sciences*. 12(10): 4889. Doi: https://doi.org/10.3390/app12104889.

[4] You, R., Lin, C.H., Wei, D., Chen, Q. 2019. Evaluating the Commercial Airliner Cabin Environment with Different Air Distribution Systems. *Indoor Air*. 29(5): 840–853. Doi: https://doi.org/10.1111/ina.12578.

[5] ASHRAE. 2019. *ASHRAE Handbook HVAC Applications*, SI., H. E. Kennedy, Ed. Mark S. Owen, 2019.

[6] Li, J., Cao, X., Liu, J., Wang, C., Zhang, Y. 2015. Global Airflow Field Distribution in a Cabin Mock-up Measured via Large-scale 2D-PIV. *Building and Environment*. 93: 234–244. Doi: https://doi.org/10.1016/j.buildenv.2015.06.030.

[7] Zhang, Y., Liu, J., Pei, J., Li, J., Wang, C. 2017. Performance Evaluation of Different Air Distribution Systems in an Aircraft Cabin Mockup. *Aerospace Science and Technology*. 70: 359–366. Doi: https://doi.org/10.1016/j.ast.2017.08.009.

[8] Liu, M., Liu, J., Cao, Q., Li, X., Liu, S., Ji, S., Lin, C. H., Wei, D., Shen, X., Long, Z., Chen, Q. 2022. Evaluation of different Air Distribution Systems in a Commercial Airliner Cabin in Terms of Comfort and COVID-19 Infection Risk. B*uilding and Environment*. 208: 108590. Doi: https://doi.org/10.1016/j.buildenv.2021.108590.

[9] Wang, A., Zhang, Y., Sun, Y., Wang, X. 2008. Experimental Study of Ventilation Effectiveness and Air Velocity Distribution in an Aircraft Cabin Mockup. *Building and Environment*. 43(3): 337–343. Doi: https://doi.org/ 10.1016/j.buildenv.2006.02.024.

[10] Wang, C., Zhang, J., Chao, J., Yang, C., Chen, H. 2022. Evaluation of Dynamic Airflow Structures in a Single-aisle Aircraft Cabin Mockup based on Numerical Simulation. *Indoor and Built Environment*. 31(2): 398–413. Doi: https://doi.org/10.1177/1420326X21992094.

[11] You, R., Chen, J., Shi, Z., Liu, W., Lin, C.H., Wei, D., Chen, Q. 2016. Experimental and numerical study of airflow distribution in an aircraft cabin mock-up with a gasper on. *Journal of Building Performance Simulation*. 9(5): 555–566. DOI: https://doi.org/10.1080/19401493.2015.1126762.

[12] Han, Y., Zhang, Y., Gao, Y., Hu, X., Guo, Z. 2022. Vortex Structure of Longitudinal Scale Flow in a 28-row Aircraft Cabin. *Building and Environment*. 222: 109362. Doi: https://doi.org/10.1016/j.buildenv.2022.109362.

[13] Hu, X., Zhang, Y., Gao, Y., Han, Y., Guo, Z. 2022. Study of the Airflow and Vortex Distributions in a Long-narrow Enclosed Space. *Science and Technology for the Built Environment*. 28(5): 690–704. Doi: https://doi.org/10.1080/23744731.2022.2044185.

[14] Cao, Q., Liu, M., Li, X., Lin, C.H., Wei, D., Ji, S., Zhang, T. T., Chen, Q. 2022. Influencing Factors in the Simulation of Airflow and Particle Transportation in Aircraft Cabins by CFD. *Building and Environment*. 207: 108413. Doi: https://doi.org/10.1016/j.buildenv.2021.108413.

[15] Sarmin, S. A. 2023. CFD Simulation and Validation for Mixing Ventilation Scaled-down Empty Aircraft Cabin using Openfoam. J*urnal Teknologi*. 85(5): 191–200. Doi: https://doi.org/10.11113/jurnalteknologi.v85.19423.

[16] Thysen, J. H., van Hooff, T., Blocken, B., van Heijst, G. 2022. PIV Measurements of Opposing-jet Ventilation Flow in a Reduced-scale Simplified Empty Airplane Cabin. *European Journal of Mechanics-B/Fluids*. 94: 212–227. Doi: https://doi.org/10.1016/j.euromechflu.2022.03.001.

[17] Thysen, J. H. 2022. Experimental and Numerical Analysis of Isothermal Opposing-jet Flows: Towards Improved Airplane Cabin Mixing Ventilation Efficiency.

[18] Thysen, J. H., van Hooff, T., Blocken, B., Van Heijst, G. J. F. 2021. CFD Simulations of Two Opposing Plane Wall Jets in a Generic Empty Airplane Cabin: Comparison of RANS and LES. *Building and Environment*. 205: 108174. Doi: https://doi.org/10.1016/j.buildenv.2021.108174.

[19] Launder, B.E., Sharma, B.I. 1974. Application of the Energy-Dissipation Model of Turbulence to the Calculation of Flow Near a Spinning Disc. *Letters in Heat and Mass Transfer*. 1(2): 131–137. Doi: https://doi.org/10.1016/0094-4548(74)90150-7.

[20] Li, X., Li, D., Yang, X., Yang, J. 2003. Total Air Age: An Extension of the Air Age Concept. *Building and Environment*. 38(11): 1263–1269. Doi: https://doi.org/

10.1016/S0360-1323(03)00133-1.

[21] Kosutova, K., van Hooff, T., Vanderwel, C., Blocken, B., Hensen, J. 2019. Cross-ventilation in a Generic Isolated Building Equipped with Louvers: Wind-tunnel Experiments and CFD Simulations. *Building and Environment*. 154: 263–280.
Doi: https://doi.org/10.1016/j.buildenv.2019.03.019.

[22] Bartak, M., Cermak, M., Clarke, J. A., Denev, J., Drkal, F., Lain, M., Macdonald, I.A., Majer, M. Stankov, P. 2001. Experimental and Numerical Study of Local Mean Age of Air.

[23] Van Hooff, T., Blocken, B., Defraeye, T., Carmeliet, J. V.,Van Heijst, G. J. F. 2012. PIV Measurements and Analysis of Transitional Flow in a Reduced-scale Model: Ventilation by a Free Plane Jet with Coanda Effect. *Building and Environment*. 56: 301–313.
Doi: https://doi.org/10.1016/j.buildenv.2012.03.020.